Check for updates

Apoptotic volume decrease (AVD) in A_{549} cells exposed to water-soluble fraction of particulate matter (PM_{10})

M. E. Giordano[1]*, G. Udayan[1], M. R. Guascito[1], A. R. De Bartolomeo[1], A. Carlino[1], M. Conte[2], D. Contini[3] and M. G. Lionetto[1,4]*

[1]Department Biological and Environmental Sciences and Technologies (DiSTeBA), Salento University, Lecce, Italy, [2]Institute of Atmospheric Sciences and Climate, ISAC-CNR, Rome, Italy, [3]Institute of Atmospheric Sciences and Climate, ISAC-CNR, Lecce, Italy, [4]NBFC, National Biodiversity Future Center, Palermo, Italy

Exposure to atmospheric particulate matter (PM) is recognized as a human health risk factor of great concern. The present work aimed to study the cellular mechanisms underlying cytotoxic effects of airborne particulate matter <10 μm in size (PM_{10}), sampled in an urban background site from January to May 2020, on A549 cells. In particular, the study addressed if PM_{10} exposure can be a main factor in the induction of the Apoptotic Volume Decrease (AVD), which is one of the first events of apoptosis, and if the generation of intracellular oxidative stress can be involved in the PM_{10} induction of apoptosis in A549 cells. The cytotoxicity of PM_{10} samples was measured by MTT test on cells exposed for 24 h to the PM_{10} aqueous extracts, cell volume changes were monitored by morphometric analysis of the cells, apoptosis appearance was detected by annexin V and the induction of intracellular oxidative stress was evaluated by the ROS sensitive $CM\text{-}H_2DCFDA$ fluorescent probe. The results showed cytotoxic effects ascribable to apoptotic death in A549 cells exposed for 24 h to aqueous extracts of airborne winter PM_{10} samples characterized by high PM_{10} value and organic carbon content. The detected reduced cell viability in winter samples ranged from 55% to 100%. Normotonic cell volume reduction (ranging from about 60% to 30% cell volume decrease) after PM_{10} exposure was already detectable after the first 30 min clearly indicating the ability of PM_{10}, mainly arising from biomass burning, to induce Apoptotic Volume Decrease (AVD) in A549 cells. AVD was prevented by the pre-treatment with 0.5 mM SITS indicating the activation of Cl^- efflux presumably through the activation of VRAC channels. The exposure of A549 cells to PM_{10} aqueous extracts was able to induce intracellular oxidative stress detected by using the ROS-sensitive probe $CM\text{-}H_2DCFDA$. The PM_{10}-induced oxidative stress was statistically significantly correlated with cell viability inhibition and with apoptotic cell shrinkage. It was already evident after 15 min exposure representing one of the first cellular effects caused by PM exposure. This result suggests the role of oxidative stress in the PM_{10} induction of AVD as one of the first steps in cytotoxicity.

KEYWORDS

AVD, particulate matter, apoptosis, A549 cells, oxidative stress, air pollution

1 Introduction

World Health Organization (WHO) recognizes that air pollution is a critical risk factor for noncommunicable diseases (NCDs) all over the world. It is estimated that air pollution is causing 24% of global adult deaths from heart disease, 25% from stroke, 43% from chronic obstructive pulmonary disease, and 29% from lung cancer. Air pollution is a major risk factor for pneumonia, being the leading cause of death in under 5 years aged children (WHO, 2019). In particular, the particulate component of air pollution poses a major risk to health. Atmospheric particulate matter (PM) is a complex mixture of components with great variability in their physical-chemical properties according to climatic, geographical, and source-specific variables (Amato et al., 2016; Chirizzi et al., 2017). The size of particles is directly linked to their potential for causing health problems. Small particles less than 10 μm in diameter pose the greatest problems because they can get deep into the respiratory tract, and some may even get into the bloodstream, in particular fine inhalable particles. According to WHO, exposure to PM has been identified as an important risk factor for mortality (WHO, 2019). The International Agency for Research on Cancer (IARC) has classified particulate matter from outdoor air pollution as carcinogenic to humans (IARC Group 1) (Loomis et al., 2013).

Although exposure to PM is recognized as a human health risk factor, the causal relationship between PM exposure and the genesis of pathological conditions and the underlying toxicological mechanisms are to date not completely understood. Several studies outlined the oxidative potential of PM (Chirizzi et al., 2017; Romano et al., 2020) and its capability to induce intracellular oxidative stress (Lionetto et al., 2019; Lionetto et al., 2021), as an important property for the outcome of adverse health effects (Cheng et al., 2016). In general, oxidative stress has been associated with cell homeostasis imbalance, mitochondrial damage, and apoptosis –(Yang et al., 2018; Zhang et al., 2018). Though numerous studies have focused on the cytotoxic effects of PM so far, several issues remain unclarified, particularly those related to the cell death pathways and underlying mechanisms (Chen et al., 2023).

Exposure to PM is known to be associated with apoptosis induction in several cell types including bone marrow (BM)-derived endothelial progenitor cells (Cui et al., 2015) through oxidative stress induction, human epithelial lung cells (L132) through activation of both TNF-α induced pathway and mitochondrial pathway (Dagher et al., 2006), mice bronchial epithelium cells via PI3K/AKT/mTOR signaling pathway (Han and Zhuang, 2021), GC-2spd cells by activation of RIPK1 apoptotic signaling pathway (Zhang et al., 2018), alveolar macrophages (Wei et al., 2021), and human cardiomyocytes (AC16 cell) (Yang et al., 2018) through mitochondria-mediated apoptosis pathway.

The apoptotic process is associated with a distinct set of molecular and cellular changes involving the cytoplasm, nucleus, and plasma membrane, which include cell shrinkage, formation of apoptotic bodies, chromatin condensation, and DNA degradation. The apoptotic cell shrinkage is a universal prominent feature of the cell under apoptosis and arises in two distinct phases: The first phase starts before cell fragmentation or formation of the apoptotic body, while the second phase is associated with cell fragmentation (Benson et al.,

1996). The early phase, called Apoptotic Volume Decrease (AVD) (Maeno et al., 2000), is represented by an isotonic cell shrinkage that occurs early after apoptotic stimuli, before the activation of caspases, the release of cytochrome c from mitochondria and DNA fragmentation, and seems to be a prerequisite for apoptosis (Okada et al., 2001). In a variety of cell types, prevention of AVD inhibits subsequent apoptotic biochemical and morphological events, and cells are rescued from death (Maeno et al., 2000; Antico et al., 2023).

The cell volume reduction during apoptosis occurs under normotonic conditions, independent of changes in the osmolarity of the extracellular environment, and is the consequence of an exit of Cl^- and K^+ from the cells (Bortner and Cidlowski, 2002; Lionetto et al., 2010; Poulsen et al., 2010; Antico et al., 2023) through the activation of specific channels. Concerning Cl^- exit from the cell, volume-regulated anion channels (VRAC) are considered the players in vertebrate cells (Maeno et al., 2000; D'Anglemont de Tassigny et al., 2004). These channels are formed by a hexameric assembly of members of the LRRC8 gene family and are ubiquitously expressed in all vertebrate cells being involved in cell volume homeostasis (Bertelli et al., 2021). The molecular mechanisms underlying their activation have not yet been completely understood. The proposed molecular mechanisms include low intracellular ionic strength, membrane unfolding, oxidation, phosphorylation, and G-protein coupling (Bertelli et al., 2021). It is known that VRAC activation is crucial to AVD happening and it occurs rapidly in a wide variety of cell types in both mitochondrion-mediated intrinsic, and death receptor-mediated extrinsic apoptosis (Maeno et al., 2000; Shimizu et al., 2004; Lee et al., 2007). Inhibition of these channels was found to prevent AVD and subsequent downstream apoptotic steps (Okada et al., 2006).

The present work aimed to study the mechanisms underlying cytotoxic effects of airborne particulate matter <10 μm in size (PM_{10}) in A549 cells, used as a model, focusing on one of the earliest events of apoptosis, the Apoptotic Volume Decrease (AVD). A549 cells are representative of the human lung Alveolar Type II pneumocytes (Foster et al., 1998), and are being widely used as a cellular model for respiratory research and assessment of adverse effects of PM on human health (Yi et al., 2012; Wang et al., 2013). Type II cells are the only cells involved in surfactant secretion in the respiratory epithelium and their damage can affect the lung defense system against environmental stressors (Akella and Deshpande, 2013).

For the study, we used aqueous extracts of eight airborne PM_{10} samples, collected in an urban site (Aradeo, province of Lecce, Puglia, Italy) potentially influenced by the local urban activities, biomass burning, agricultural activities, and the nearby industrial activities during the period from 14-01-2020 to 28-05-2020. Guascito et al. (2023) described that the larger contribution of PM_{10} in the study site originated from biomass burning.

The choice of water-soluble extracts of sampled PM_{10} arises from the experimental need to reproduce experimental conditions similar to the physiological exposure at the level of respiratory epithelium, where the surface of the respiratory epithelial cells is covered by a thin fluid layer, in which PM_{10} dissolves.

To the best of our knowledge, this is the first work focusing on airborne PM and AVD induction and aims to contribute to improving the knowledge about the mechanisms underlying the effects of PM at the airway epithelium.

2 Materials and methods

2.1 Sampling campaign, PM$_{10}$ gravimetric determination and chemical composition

The study was performed on eight PM$_{10}$ samples chosen from the whole sampling campaign carried out from December to May 2020 in a site located in southeastern Italy (Aradeo, Puglia, Italy) already described in a previous work (Guascito et al., 2023). The sampling site was located in the center of the municipality of Aradeo (Lecce, Italy) ($40°07'47''$ N; $18°07'56''$ E) with a population of about 10,000 inhabitants. The site is an urban background site potentially influenced by the local urban activities, biomass burning and agricultural activities, and the nearby industrial activities including a cement production plant located at about 7.2 km in the northeast direction. Daily PM$_{10}$ samples (starting from midnight) were collected by an automatic low-volume sampler at 38.3 L·min^{-1} (Zambelli Explorer Plus) on PFTE filters (Whatman, 47 mm in diameter) located on the roof of the City Hall at about 14 m above the ground.

As widely described by Guascito et al. (2023), the larger contribution of PM$_{10}$ in the study site originated from biomass burning.

Gravimetric determination of PM$_{10}$ samples was done according to UNI EN 12341 (2014) by weighing the filters (three replicates before and after sampling), following stabilization for 48 h in a conditioned room (for details see Guascito et al., 2023). The weighing was performed using a microbalance Sartorious Cubis (model MSx6.6S, ±1 μg resolution). Quality control of gravimetric results was done using field blanks and periodic (once per week) control of the inlet flow rate of the samplers with external flow meters. Organic (OC) and elemental carbon (EC) were determined by a Sunset laboratory carbon analyser (Sunset Laboratory Inc., Tigard OR, United States) using thermo-optical transmittance (TOT) with the EUSAAR2 protocol (Cesari et al., 2018). The analyser was calibrated using a sucrose solution as an external standard (2.198 g/L in water, CPAchem Ltd., Bulgaria). Linear calibration had a slope of 0.97 (±0.01), a negligible intercept, (0.1 ± 0.2), and a determination coefficient R^2 = 0.99.

The chemical composition of PM$_{10}$ sampled was determined via ICP-MS (PerkinElmer NexION 1000 and NexION 300x) for the main metals and ion chromatography (ICS1100, Thermo Scientific) for the water-soluble ions according to Guascito et al. (2023).

2.2 Cell viability measurement by MTT assay

Cell viability was evaluated by MTT test on A549 cells exposed for 24 h to the water-soluble fractions of PM$_{10}$ extracted from the whole PFTE filter for each of the eight samples according to Lionetto et al. (2021). Extraction was carried out in 10 mL ultrapure water (Milli-Q) using an ultrasonic bath. Four cycles of sonication for a total of 80 min were performed and each cycle was followed by 1 min vortex agitation (according to Lionetto et al., 2021). Then, the extracts were filtered using PTFE (polytetrafluoroethylene) 0.45 μm pore syringe filters. The assay measures the metabolic activity of the cells as an indicator of cell viability, assessing the mitochondrial NAD(P)H-dependent oxidoreductase enzyme activity which

reduces a yellow tetrazolium salt (3-(4,5-dimethylthiazol-2-yl)-2,5-diphenyltetrazolium bromide (MTT) 3-(4, 5-dimethylthiazol-2-yl)-2, 5-diphenyltetrazolium bromide to formazan that accumulates as crystals within healthy cells. These are dissolved with DMSO and the absorbance of the resulting colored solution is spectrophotometrically analyzed at 570 nm (Cytation 5, BioTek Instruments, Winooski, VT, United States). Six replicates per sample were carried out. The relative viability of the cells was calculated as follows:

$$\text{Relative viability of cells (\%)} = \left[(\text{treated cells OD}) / \right.$$
$$\left. \times (\text{untreated cells OD}) \right] \times 100$$

2.3 Morphological analysis of the cells and cell volume change determination

A549 cells adherent to the bottom of a 96 multiwell were exposed to the PM$_{10}$ aqueous extracts for 24 h and visualized by Cytation 5 cell imaging multimode reader (Agilent, Santa Clara, CA, United States) (observation objective: ×40). Cell volume changes were monitored by morphometric analysis of the cells and were expressed as a percentage of the cell area of 2-D cell images after PM$_{10}$ exposure vs. the cell area of control cells (cells not exposed to the PM$_{10}$ extracts) according to Giordano et al. (2020) and Lionetto et al. (2010). At least a minimum of 100 cells/field and 5 fields per well were analyzed.

2.4 Detection of apoptosis by annexin V

One of the earliest events of apoptosis is the translocation of the membrane phospholipid from the inner to the outer leaflet of the plasma membrane. Once exposed to the extracellular environment, binding sites on phosphatidylserine become available for Annexin V, a 36 kDa Ca^{2+}-dependent phospholipid-binding protein that has a high affinity for the anionic phospholipid phosphatidylserine (Leventis and Grinstein, 2010).

A549 cells exposed to PM$_{10}$ aqueous extracts for 24 h were incubated with 1 μg/mL annexin V (Alexa Fluor® 488) for 15 min and viewed by Cytation 5 cell imaging multimode reader according to Gelles et al. (2019).

2.5 Intracellular oxidative stress detection assay and confocal visualization

The intracellular oxidative stress was assessed using the ROS-sensitive cell-permeant probe 5-(6)-Chloromethyl-2′,7′-dichlorodihydrofluorescein diacetate, acetyl ester (CMH$_2$DCFDA) (Ex/Em: 492–495/517–527 nm) (Thermo Fisher Scientific, Waltham, MA, United States) according to Lionetto et al. (2021); Giordano et al. (2020). The probe, once in the intracellular compartment, loses its acetate group, which is cleaved by cellular esterases, and undergoes hydrolysis. The resulting DCFH carboxylate anion is trapped inside the cell and once oxidized by intracellular ROS produces the fluorescent product DCF

TABLE 1 Values of PM$_{10}$ concentrations and carbon content (organic carbon OC and elemental carbon EC) of the eight samples used for the study.

Sampling data	PM$_{10}$ (µg/m³)	OC (µg/m³)	EC (µg/m³)
14/1/2020	47.9 ± 2.4	29.6 ± 1.5	3.2 ± 0.2
18/1/2020	50.8 ± 2.5	21.8 ± 1.1	2.0 ± 0.1
21/1/2020	37.9 ± 1.9	17.8 ± 0.9	1.9 ± 0.1
23/1/2020	35.4 ± 1.8	4.6 ± 0.3	0.4 ± 0.1
11/2/2020	27.1 ± 1.3	4.7 ± 0.3	0.5 ± 0.1
5/3/2020	27.9 ± 1.4	11.6 ± 0.6	1.3 ± 0.1
9/5/2020	14.1 ± 0.7	3.3 ± 0.2	0.4 ± 0.1
28/5/2020	12.9 ± 0.6	2.6 ± 0.2	0.3 ± 0.1

FIGURE 1
Cytotoxicity of PM$_{10}$ expressed as % cell viability inhibition assessed by the MTT test on A549 cells exposed for 24 h to PM$_{10}$ aqueous extracts.

(Ameziane-El-Hassani and Dupuy, 2013). Fluorescence intensity was measured using the Cytation 5 cell imaging multimode reader. The results were expressed as a fold increase in the fluorescence intensity compared to the negative control (untreated cells). More details of the methodology are reported in Giordano et al. (2020).

Cells charged with CM-H$_2$DCFDA were also visualized by confical microscopy. Briefly, A549 cells were plated at a density of 1×10^5 cells per mL into a chambered coverslip (IBIDI, Gräfelfing, Germany), incubated for 24 h for the adhesion of the cells to the bottom of the plate, then exposed for 24 h with the aqueous PM$_{10}$ extracts and finally charged with CM-H$_2$DCFDA as reported above. The cells were viewed using a ×100 NA plan apochromatic objective mounted on a NIKON TE300 inverted microscope coupled to a NIKON C1 confocal laser scanning unit (Nikon, Tokyo, Japan). The Argon 488-nm laser line was used. Unlabeled cells did not exhibit any detectable fluorescence under the conditions used. Images were acquired and analyzed by EZ-C1 NIKON software.

2.6 Statistics

Data are given as the mean ± S.E.M. The statistical significance was analyzed by one-way ANOVA, and Dunnett's multiple comparison test.

3 Results

3.1 Effect of PM$_{10}$ exposure on cell viability

The average values of PM$_{10}$ concentration and carbon content of the 8 samples used in the present study are reported in Table 1. The sample set included six winter samples characterized by higher PM$_{10}$ concentrations and two spring samples characterized by lower PM$_{10}$ values in agreement with the typical seasonal PM$_{10}$ concentration of the area (Cesari et a., 2018). On average the same trend was also observed for carbon content. Moreover, it must be considered that the sampling campaign was carried out in 2020, when Italy was subjected to a national lockdown and limitation to the movement of people because of the COVID-19 pandemic. The first six samples were collected before the lockdown period, while the other two May
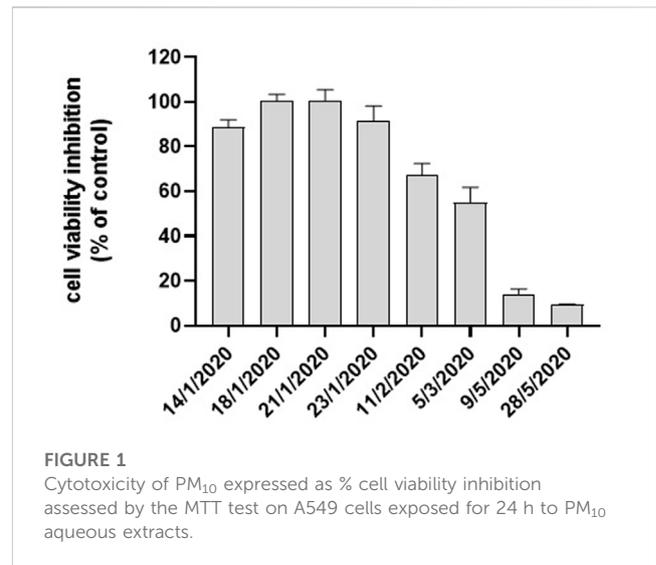
samples were collected just after the lockdown when the restart of activities was slow. Some previous evidence indicated that the lockdown has slightly reduced the PM$_{10}$ concentration in the air at least in this region of Italy (Dinoi et al., 2021). The mean chemical composition of the PM$_{10}$ in the study site is reported in Supplementary Table S1.

Cell viability after 24 h exposure to water-soluble extract of the airborne PM$_{10}$ samples was assessed by MTT assay on A549 cells. In Figure 1 the MTT results obtained on the eight PM$_{10}$ samples chosen for the objective of the present study are reported. Inhibition of the mitochondrial NAD(P)H-dependent cellular oxidoreductase enzymatic activity after exposure of A549 cells for 24 h to the aqueous extracts of PM$_{10}$ compared to control cells was observed in the sample data set in agreement with a previous study on the whole sampling campaign (Guascito et al., 2023). The entity of the inhibition varied from about 100% (detected in January samples) to values of about 9% recorded in May samples. The dose-dependence response of the assay for each aqueous extract was preliminarily checked by exposure of A549 cells to increasing dilutions of the same extract, as reported in our previous studies (Lionetto et al., 2019; Lionetto et al., 2021). On average, winter samples showed a higher cytotoxic potential as indicated by the high percentage reduction of cell viability, particularly in January and February, compared to the two May samples according to Guascito et al. (2023) in parallel to PM$_{10}$ concentration.

3.2 Cell volume alteration and apoptosis detection in A549 cells exposed to PM$_{10}$

To deepen the analysis of the mechanisms involved in PM$_{10}$-induced cytotoxicity on A549 cells, cell morphology was analyzed on PM$_{10}$ exposed cells in parallel to MTT assay using Cytation 5 cell imaging multimode reader on the same samples.

After 24 h exposure to PM$_{10}$ aqueous extracts, A549 cells showed typical cell shrinkage detected as a percentage decrease of the cell area of 2-D images compared to not exposed (control) cells (Figure 2A). Cell shrinkage levels were in agreement with the
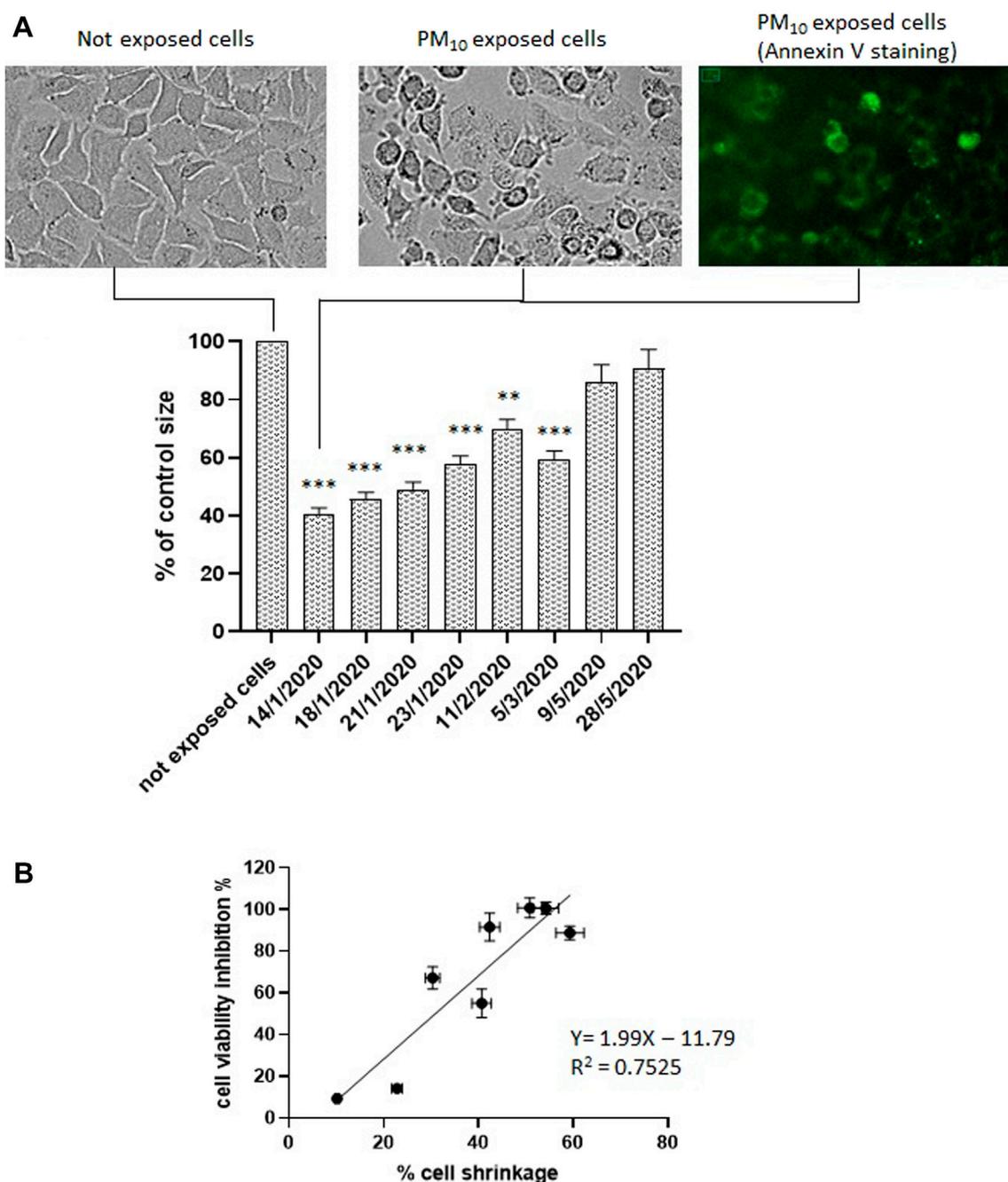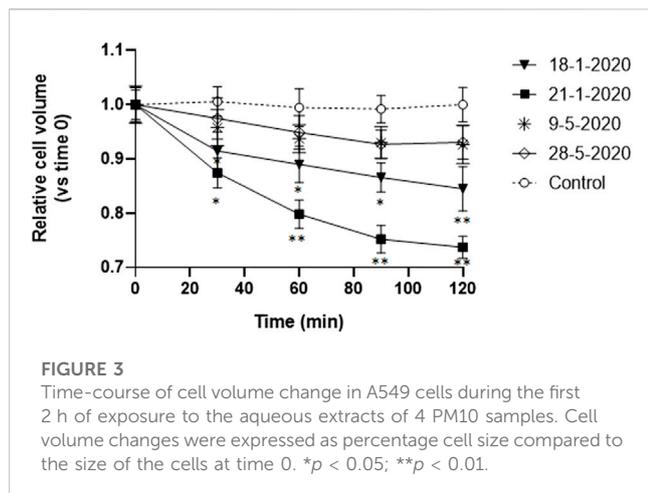
FIGURE 2
(A, B) Cell volume change in A549 cells exposed to the aqueous extracts of the 8 PM10 samples expressed as percentage cell size compared to not exposed cells (control). Representative brightfield image of not exposed cells; representative images of PM$_{10}$ exposed cells (sample of 14-1-2020). brightfield and annexin V stained. (B) Correlation analysis between cell viability inhibition and % of cell shrinkage.

NAD(P)H-dependent cellular oxidoreductase enzymatic activity reduction, as indicated by the correlation analysis (Figure 2B). Particularly high cell volume reduction, above 50%, was observed in the samples which showed the highest inhibition of mitochondrial NAD(P)H-dependent oxidoreductase activity. Cell shrinkage was also accompanied by other typical morphological signs of apoptosis such as cell rounding, surface roughness, blebs formation, and annexin V positivity, visualized by the delectable green contour of the cell plasma membrane of cells treated with 1 µg/mL annexin V (Alexa Fluor® 488) following exposure to PM$_{10}$ extract as shown in Figure 2A. This figure reports representative images obtained from the sample of 14-1-2020. Similar apoptotic positive evidence (cell rounding, surface roughness, blebs formation, and annexin V positivity) were obtained also for the other 5 winter samples but was not detectable for the two May samples (not shown).

FIGURE 3
Time-course of cell volume change in A549 cells during the first 2 h of exposure to the aqueous extracts of 4 PM10 samples. Cell volume changes were expressed as percentage cell size compared to the size of the cells at time 0. *$p < 0.05$; **$p < 0.01$.

3.3 Apoptotic volume decrease in A549 cells exposed to PM$_{10}$ aqueous extracts
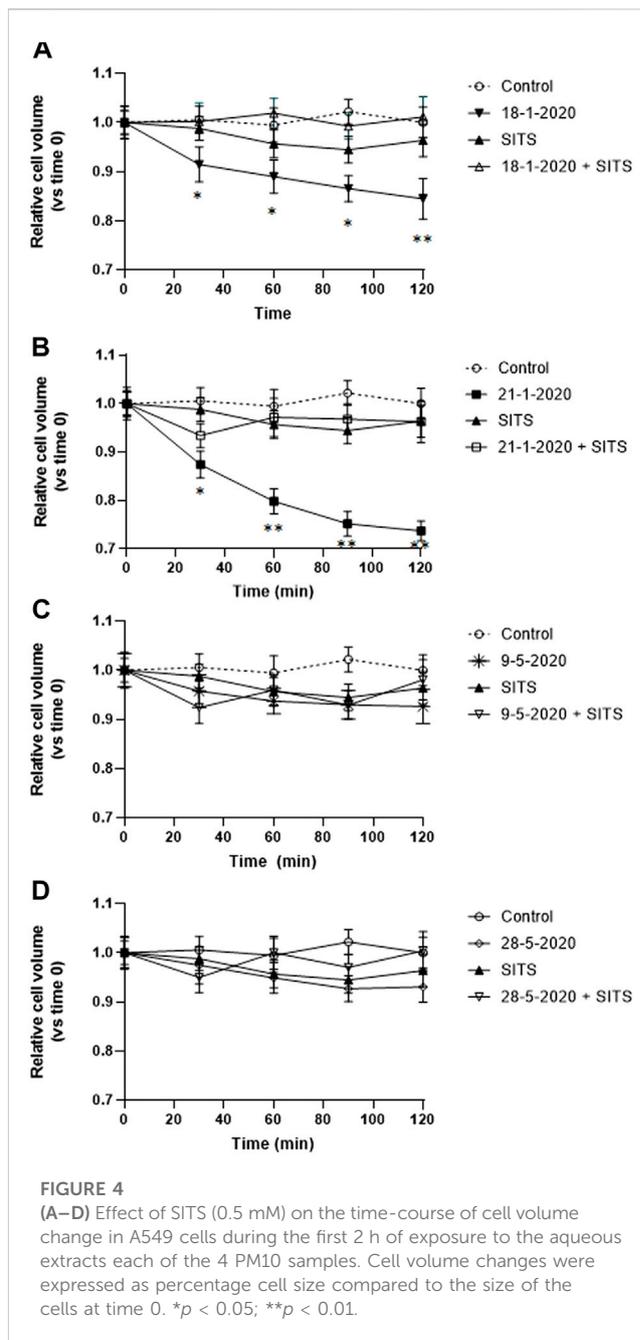
After detecting reduced vitality and apoptosis appearance in A549 cells following 24 h exposure to PM$_{10}$ aqueous extracts, we tested the hypothesis of the possible involvement of PM$_{10}$ exposure in the induction of the Apoptotic Volume Decrease (AVD), which is one of the first events of apoptosis, occurring early in the first 1–2 h (Chang et al., 2000; Maeno et al., 2000). Therefore, the time course of the volume changes was monitored in A549 cells during the first 2 h of exposure to PM$_{10}$ aqueous extracts by time-lapse imaging of the cells every 30 min. The AVD analysis was focused on 4 representative samples, two January samples, characterized by the highest values of vitality reduction and a marked cell shrinkage after 24 h exposure, and the two samples of May, characterized by a reduction of the NAD(P)H-dependent cellular oxidoreductase activity below 15% and without apparent apoptotic signs. For each of the four filter extracts, three independent experiments were performed.

The cells exposed to the aqueous extracts of January 18 and 21 showed a significant reduction of cell volume compared to control cells already after 30 min exposure and the decrease continued in the 2 h observation reaching 16% and 27% respectively (Figure 3). If these results are compared with the overall apoptotic cell volume reduction observed after 24 h in the same extracts, the AVD response observed in the first 2 h corresponds to one-third and one-half respectively of the overall cell shrinkage produced.
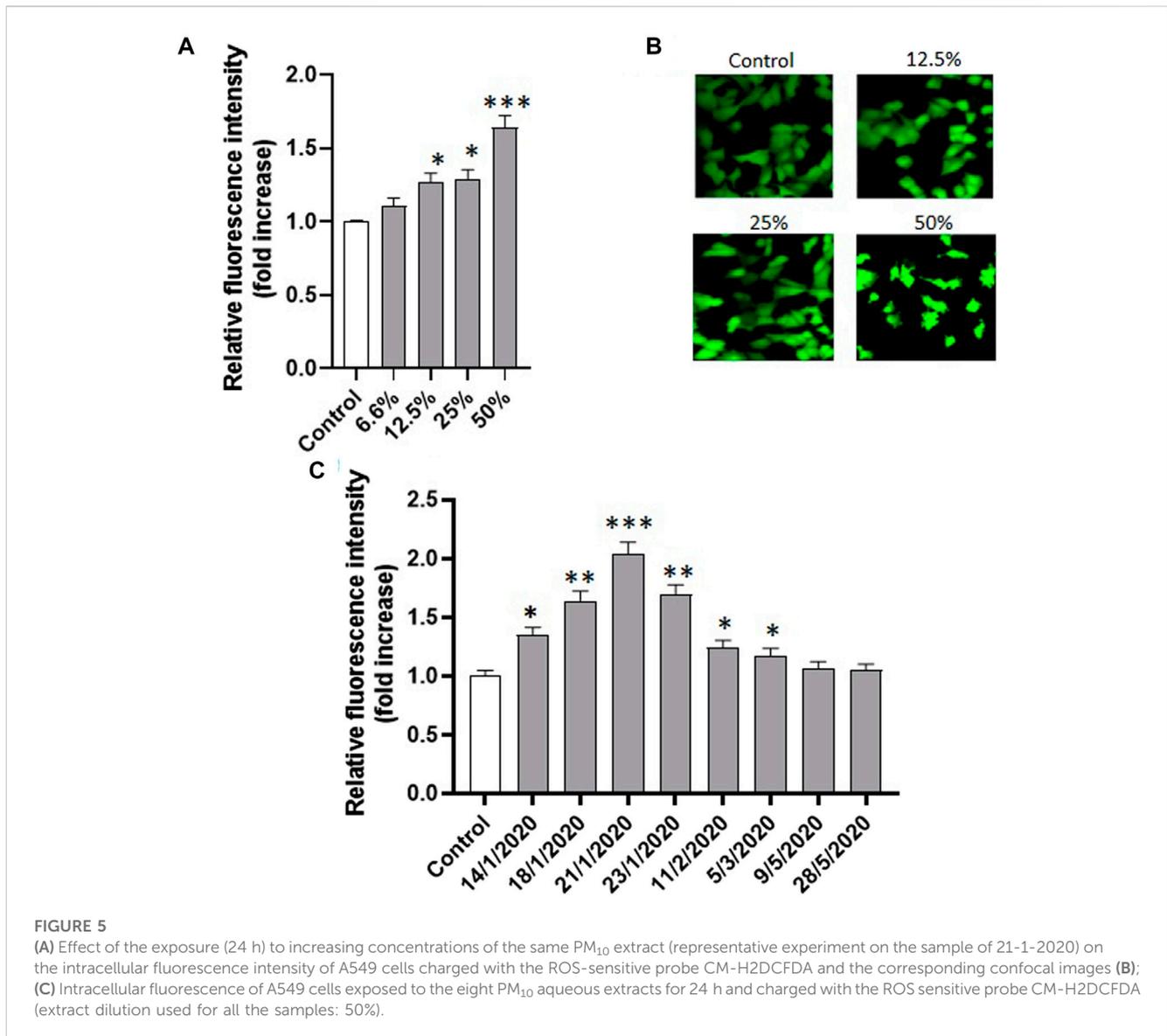
On the other hand, the cells exposed to the other two spring extracts (9-5-2022 and 28-5-2022) did not show any significant cell size reduction compared to the control cells.

3.4 Effect of SITS in the PM$_{10}$-induced apoptotic volume decrease

AVD is known to be caused by the loss of K$^+$ and Cl$^-$ from the cell (Yu and Choi, 2000). Therefore, in order to investigate the nature of the PM$_{10}$-induced early isotonic cell shrinkage, A549 cells were preincubated with 0.5 mM disulfonic stilbene

FIGURE 4
(A–D) Effect of SITS (0.5 mM) on the time-course of cell volume change in A549 cells during the first 2 h of exposure to the aqueous extracts each of the 4 PM10 samples. Cell volume changes were expressed as percentage cell size compared to the size of the cells at time 0. *$p < 0.05$; **$p < 0.01$.

derivative (4-Acetamido-40-isothiocyanato-stilbene-2,20-disulfonic acid), a known inhibitor of Cl$^-$ channels (Kokubun et al., 1991) including the ubiquitously expressed volume-regulated anion channels (VRACs) (Maeno et al., 2000; Hoffman et al., 2015; Okada et al., 2021), which have been demonstrated to be involved in AVD in other cell types (Maeno et al., 2000). The cells were viewed by time-lapse microscopy. After (4-Acetamido-40-isothiocyanato-stilbene-2,20-disulfonic acid) preincubation, the cells were exposed to the PM$_{10}$ aqueous extracts of 18-1-2020 and 21-1-2020 for 2 h and in this case, the PM-induced isotonic shrinkage was completely prevented (Figures 4A, B). On the other hand, (4-Acetamido-40-isothiocyanato-stilbene-2,20-disulfonic acid)

FIGURE 5
(A) Effect of the exposure (24 h) to increasing concentrations of the same PM_{10} extract (representative experiment on the sample of 21-1-2020) on the intracellular fluorescence intensity of A549 cells charged with the ROS-sensitive probe CM-H2DCFDA and the corresponding confocal images **(B)**; **(C)** Intracellular fluorescence of A549 cells exposed to the eight PM_{10} aqueous extracts for 24 h and charged with the ROS sensitive probe CM-H2DCFDA (extract dilution used for all the samples: 50%).

alone was not able to produce any significant alteration in cell size. The other two extracts, not showing AVD, were also tested and no significant effect of (4-Acetamido-40-isothiocyanato-stilbene-2,20-disulfonic acid) treatment was observed (Figures 4C, D).
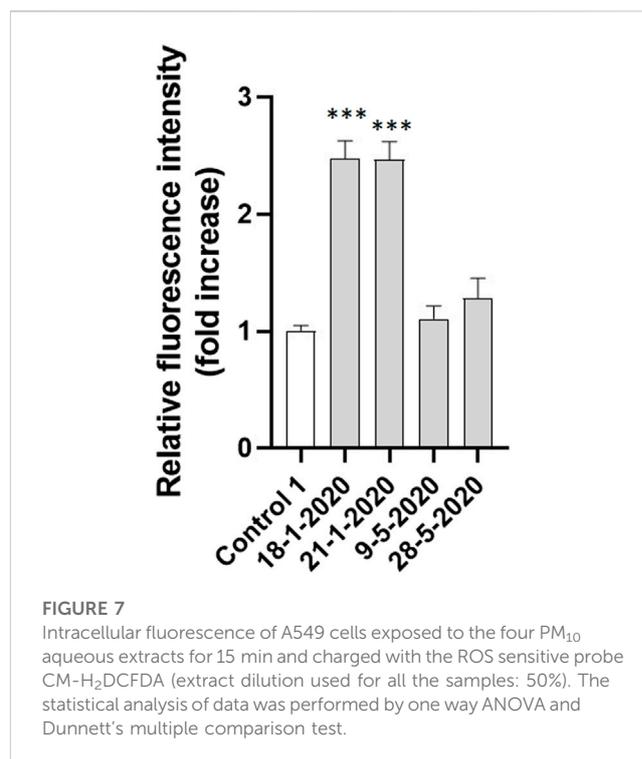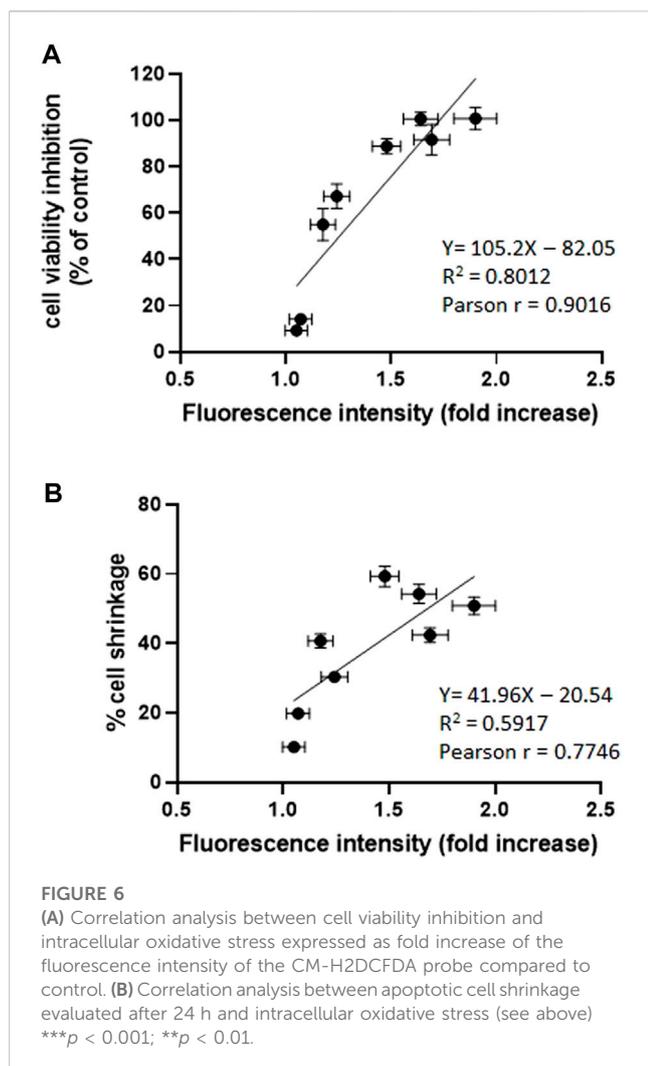
3.5 Oxidative stress induction in A549 cells exposed to PM_{10}

It is known that reactive oxygen species and oxidative stress play a pivotal role in apoptosis induction in several cell types (Kannan and Jain, 2000; Redza-Dutordoir and Averill-Bates, 2016).

In order to test whether oxidative stress was involved in PM_{10}-induced apoptosis in A549 cells, intracellular oxidative stress levels were measured in A549 exposed for 24 h to all the

eight PM_{10} aqueous extracts of the study using the cell-permeable probe CM-H_2DCFDA. Preliminarily, the cells were exposed to different dilutions of the same extract. Figure 5A shows the representative dose response for one of the tested samples (21-1-2021) revealing that PM_{10} was able to induce the generation of intracellular oxidative stress in a dose-dependent way. The confocal representative images of cells exposed to different dilutions of the PM_{10} extracts and then charged with the fluorescent probe are reported in Figure 5B. The intracellular fluorescence intensity of the exposed cells increases with the concentration of the PM_{10} aqueous extract. At the highest dilution tested the appearance of apoptotic blebs is clearly evident.

The analysis of the PM_{10}-induced intracellular oxidative stress was applied to the eight extracts revealing a highly significant fluorescence increase compared to control in the six winter samples after 24 h, while no significant effect was observed in the

FIGURE 6
(A) Correlation analysis between cell viability inhibition and intracellular oxidative stress expressed as fold increase of the fluorescence intensity of the CM-H2DCFDA probe compared to control. **(B)** Correlation analysis between apoptotic cell shrinkage evaluated after 24 h and intracellular oxidative stress (see above) ***$p < 0.001$; **$p < 0.01$.

FIGURE 7
Intracellular fluorescence of A549 cells exposed to the four PM_{10} aqueous extracts for 15 min and charged with the ROS sensitive probe CM-H_2DCFDA (extract dilution used for all the samples: 50%). The statistical analysis of data was performed by one way ANOVA and Dunnett's multiple comparison test.

two spring samples (Figure 5C). The oxidative stress data were statistically correlated with vitality inhibition data and cell shrinkage results (Figures 6A, B) suggesting that the generation of intracellular oxidative stress can be one of the main underlying mechanisms of the PM_{10} induction of apoptosis in A549 cells.

The investigation of the effect of PM_{10} exposure on intracellular oxidative stress induction was deepened with a short-term analysis of the intracellular fluorescence of A549 cells charged with CM-H_2DCFDA and exposed for 15 min to the 4 aqueous PM_{10} extracts used for AVD analysis. As reported in Figure 7, the cells exposed to the aqueous extracts of 18-1-2020 and 21-1-2020 expressed a significantly increased fluorescence compared to control cells already after 15 min exposure, suggesting that the induction of oxidative stress by PM_{10} was an early event, timely correspondent with the AVD induction sustained by VRAC channels.

4 Discussion

The impact of air pollution on public health has become a great concern worldwide, in particular, PM is considered one of the main risk factors for human health (Loomies et al., 2013; WHO, 2019). Cell death has been used as a hallmark of cell injury induced by PM (Peixoto et al., 2017) representing a general toxic outcome since it results from the integration of the multiple toxic effects that PM can induce at the cellular level. Cell death has been recognized as one important underlying mechanism of the development or exacerbation of respiratory diseases, such as emphysema and chronic obstructive pulmonary diseases (Pleixoto et al., 2017).

The present work wants to contribute to the knowledge about the mechanisms underlying the cytotoxic effects of PM at the airway epithelium using A549 cells as a model and focuses on the induction of apoptotic volume decrease, one of the early events in the apoptotic process. The study was carried out on water extracts of airborne PM coming from an urban site in the South of Italy (Aradeo, province of Lecce, Apulia, Italy) whose dominant PM source was represented by biomass burning during the sampling period of the study as previously assessed by Guascito et al. (2023). The used samples included winter samples with high PM_{10} values, high carbon content values (mainly linked to biomass combustion, as previously assessed), and high cytotoxicity, and spring samples, collected in the post-COVID-lockdown period, characterized by low PM_{10} values, low carbon content values, and low or negligible cytotoxicity.

Cell death has a central role in homeostasis and it is also responsible for the onset of several pathological conditions. In recent years, various types of cell death, such as apoptosis, autophagy, necrosis, pyroptosis, ferroptosis, and cuproptosis, have been elucidated (Chen et al., 2023), and an increasing number of works have focused on the cellular death pathways related to PM exposure. Among the death cell types, apoptosis is the most widely

investigated in PM-induced cytotoxicity and it has been related to the appearance of pulmonary fibrosis (Yang et al., 2020).

In our study, cytotoxic effects induced by PM_{10} ascribable to apoptotic death were observed in winter samples which are characterized by the higher PM_{10} and organic carbon content, as revealed by the typical apoptotic sign appearance such as cell volume reduction, cell rounding, surface roughness, blebs formation, and annexin V positivity. Apoptotic volume reduction was observed early, since a significant cell shrinkage was already detectable after the first 30 min exposure to the winter PM_{10} samples, while no significant changes in cell volume were observed in spring samples which did not show the typical sign of apoptosis. These results clearly indicate the ability of $PM_{10,}$ mainly arising from biomass burning, to induce AVD in A549 cells. AVD was triggered by the activation of Cl^- efflux, since the pretreatment with SITS, a known inhibitor of Cl^- channels including the VRAC channels, completely inhibited the PM-induced activation of AVD. The pretreatment with SITS did not exert any effect on cell volume in control conditions suggesting that the channels responsible for the PM_{10}-induced Cl^- efflux were not activated in basal conditions.

A549 cells are known to express the ubiquitous volume-regulated anion channels (VRAC) composed of members of the leucine-rich repeat-containing protein 8 family (LRRC8A-E) (He et al., 2010; Canella et al., 2017; Bach et al., 2018; Centeio et al., 2020). Normally, these channels are closed and underwent activation following hypotonic swelling playing a key role in the Regulatory Volume Decrease response which allows the cells to recover their volume through the release of osmolytes (mainly K^+ and Cl^-) followed by loss of osmotically obliged water. In addition, VRAC channels have been previously demonstrated to be activated in A549 cells in normotonicity under apoptosis-related stressful conditions such as carboplatin and ozone exposure (He et al., 2010; Canella et al., 2017; Bach et al., 2018) being responsible for the induction of AVD. In light of this knowledge, our results indicate the ability of biomass-burning-related PM_{10} to activate AVD in A549 cells through the activation of VRAC channels.

As regards the PM_{10} components able to induce the activation of VRAC channels, it is known that these channels are activated by ROS in various cell types (Jiao et al., 2006; Matsuda et al., 2010; Shen et al., 2014; Friard et al., 2021). PM is known to express an intrinsic oxidant-generating capacity that is related with the physical-chemical properties of the particles, such as their surface characteristics and their chemical composition, related to the pollutants adsorbed (such as metals, polycyclic aromatic hydrocarbons, quinones) expressed by the PM oxidative potential (Chirizzi et al., 2017; Carlino et al., 2023). Besides its intrinsic oxidant-generating capacity, PM also exhibits a cell-mediated oxidant-generating capacity once in the cells, including the activation of intracellular signaling pathways leading to the formation of ROS, the interference with the endogenous production of ROS at the mitochondrial level, the release of radical metabolites arising from the biotransformation of the chemical contaminants of PM (Ghio et al., 2012), and the inhibition of intracellular antioxidant defenses (Chirino et al., 2010). The two types of PM oxidant properties (endogenous and cell-mediated) are statistically correlated as previously demonstrated (Lionetto et al., 2021; Guascito et al., 2023).

In our study, we found that exposure of A549 to PM_{10} aqueous extracts was able to induce intracellular oxidative stress detected by the ROS-sensitive probe $CM-H_2DCFDA$. The oxidative stress induction, expressed as a fold increase of the intracellular probe fluorescence, was statistically significantly correlated with cell viability inhibition and with apoptotic cell shrinkage. The oxidative stress induction was already evident after 15 min exposure suggesting that the appearance of PM_{10} induced AVD through the activity of VRAC channels is mediated by the PM_{10} induced intracellular oxidative stress, which in turn represents one of the first PM-induced cellular effects leading to cytotoxicity.

5 Conclusion

In conclusion, obtained results demonstrated for the first time that exposure to airborne PM_{10} aqueous extracts, mainly influenced by biomass burning, induces Apoptotic Volume Decrease in A549 cells. AVD was prevented by the pre-treatment with SITS suggesting the activation of Cl^- efflux presumably through the activation of VRAC channels. The exposure of A549 cells to PM_{10} aqueous extracts was able to induce intracellular oxidative stress detected by using the ROS-sensitive probe $CM-H_2DCFDA$. The PM_{10} oxidative stress induction was statistically significantly correlated with cell viability inhibition and with apoptotic cell shrinkage. The oxidative stress induction was already evident after 15 min exposure representing one of the first cellular effects induced by PM exposure leading to cytotoxicity. Its early appearance suggests its role in the PM_{10} mediated AVD induction. This finding deserves to be in more detail evaluated in future works addressing the efficiency of the endogenous antioxidant system in PM treated A549 cells.

Although future studies are needed to better clarify important aspects of the research such as the signaling pathway accounting for AVD activation through VRAC opening and the role played by ROS in these pathways also in relation to the chemical composition of $PM_{10,}$ the manuscript contributes to improving the knowledge about the cellular mechanisms responsible for the effects of PM at the airway epithelium.

Data availability statement

The raw data supporting the conclusion of this article will be made available by the authors, without undue reservation.

Author contributions

Conceptualization: MEG and MGL; Methodology: MEG, and MGL; Investigation: MEG, GU, MRG, AC, MC, DC, and MGL; resources: MGL, MRG, and DC; data curation: MEG, GU, MRG, AC, MC, DC, and ML; writing–original draft preparation: MEG and ML; writing—review and editing: MEG, GU, MRG, AC, MC, DC, and ML; supervision: ML. All authors contributed to the article and approved the submitted version.

Funding

Acknowledgments

Conflict of interest

The authors declare that the research was conducted in the absence of any commercial or financial relationships that could be construed as a potential conflict of interest.

Publisher's note

All claims expressed in this article are solely those of the authors and do not necessarily represent those of their affiliated organizations, or those of the publisher, the editors and the reviewers. Any product that may be evaluated in this article, or claim that may be made by its manufacturer, is not guaranteed or endorsed by the publisher.

Supplementary material

The Supplementary Material for this article can be found online at: https://www.frontiersin.org/articles/10.3389/fphys.2023.1218687/full#supplementary-material

References

Akella, A., and Deshpande, S. B. (2013). Pulmonary surfactants and their role in pathophysiology of lung disorders. *Indian J. Exp. Biol.* 51, 5–22.

Amato, F., Alastuey, A., Karanasiou, A., Lucarelli, F., Nava, S., Calzolai, G., et al. (2016). AIRUSE-LIFE+: A harmonized PM speciation and source apportionment in five southern European cities. *Atmos. Chem. Phys.* 16, 3289–3309. doi:10.5194/acp-16-3289-2016

Ameziane-El-Hassani, R., and Dupuy, C. (2013). Detection of intracellular reactive oxygen species (CM-H_2DCFDA). *Bio-protocol* 3, e313. doi:10.21769/bioprotoc.313

Antico, S., Lionetto, M. G., Giordano, M. E., Caricato, R., and Schettino, T. (2023). Cell volume regulation and apoptotic volume decrease in rat distal colon superficial enterocytes. *Cell. Physiol. biochem.* 32, 1551–1565. doi:10.1159/000356592

Bach, M. D., Sørensen, B. H., and Lambert, I. H. (2018). Stress-induced modulation of volume-regulated anions channels in human alveolar carcinoma cells. *Physiol. Rep.* 6, e13869. doi:10.14814/phy2.13869

Benson, R. S. P., Heer, S., Dive, C., and Watson, A. J. M. (1996). Characterization of cell volume loss in CEM-C7A cells during dexamethasone-induced apoptosis. *Am. J. Physiol.* 270, C1190–C1203. doi:10.1152/ajpcell.1996.270.4.C1190

Bertelli, S., Remigante, A., Zuccolini, P., Barbieri, R., Ferrera, L., Picco, C., et al. (2021). Mechanisms of activation of LRRC8 volume regulated anion channels. *Cell Physiol. Biochem.* 55 (S1), 41–56. doi:10.33594/000000329

Bortner, C. D., and Cidlowski, J. A. (2002). Apoptotic volume decrease and the incredible shrinking cell. *Cell Death Differ.* 9, 1307–1310. doi:10.1038/sj.cdd.4401126

Canella, R., Martini, M., Borriello, R., Cavicchio, C., Muresan, X. M., Benedusi, M., et al. (2017). Modulation of chloride currents in human lung epithelial cells exposed to exogenous oxidative stress. *J. Cell Physiol.* 232, 1817–1825. doi:10.1002/jcp.25705

Carlino, A., Romano, M. P., Lionetto, M. G., Contini, D., and Guascito, M. R. (2023). An overview of the automated and on-line systems to assess the oxidative potential of particulate matter. *Atmosphere.* 14, 256. doi.org/doi:10.3390/atmos14020256

Centeio, R., Ousingsawat, J., Schreiber, R., and Kunzelmann, K. (2020). Ca^{2+} dependence of volume-regulated VRAC/LRRC8 and TMEM16A Cl^- channels. *Front. Cell. Dev. Biol.* 8, 596879. doi:10.3389/fcell.2020.596879

Cesari, D., De Benedetto, G. E., Bonasoni, P., Busetto, M., Dinoi, A., Merico, E., et al. (2018). Seasonal variability of $PM_{2.5}$ and PM_{10} composition and sources in an urban background site in Southern Italy. *Sci. Total Environ.* 612, 202–213. doi:10.1016/j.scitotenv.2017.08.230

Chang, S. H., Phelps, P. C., Berezesky, I. K., Ebersberger, M. L., and Trump, B. F., Jr. (2000). Studies on the mechanisms and kinetics of apoptosis induced by microinjection of cytochrome c in rat kidney tubule epithelial cells (NRK-52E). *Am. J. Pathol.* 156, 637–649. doi:10.1016/S0002-9440(10)64768-2

Chen, Y., Wu, Y., Qi, Y., and Liu, S. (2023). Cell death pathways: The variable mechanisms underlying fine particulate matter-induced cytotoxicity. *Nanosci* 3, 130–139. doi:10.1021/acsnanoscienceau.2c00059

Cheng, H., Saffari, A., Sioutas, C., Forman, H. J., Morgan, T. E., and Finch, C. E. (2016). Nanoscale particulate matter from urban traffic rapidly induces oxidative stress and inflammation in olfactory epithelium with concomitant effects on brain. *Environ. Health Perspect.* 124, 1537–1546. doi:10.1289/EHP134

Chirino, Y. I., Sánchez-Pérez, Y., Osornio-Vargas, Á. R., Morales-Bárcenas, R., Gutiérrez-Ruíz, M. C., Segura-García, Y., et al. (2010). PM_{10} impairs the antioxidant defense system and exacerbates oxidative stress driven cell death. *Toxicol. Lett.* 193, 209–216. doi:10.1016/j.toxlet.2010.01.009

Chirizzi, D., Cesari, D., Guascito, M. R., Dinoi, A., Giotta, L., Donateo, A., et al. (2017). Influence of Saharan dust outbreaks and carbon content on oxidative potential of water-soluble fractions of $PM_{2.5}$ and PM_{10}. *Atmos. Environ.* 163, 1–8. doi:10.1016/j.atmosenv.2017.05.021

Cui, Y., Xie, X., Jia, F., He, J., Li, Z., Fu, M., et al. (2015). Ambient fine particulate matter induces apoptosis of endothelial progenitor cells through reactive oxygen species formation. *Cell. Physiol. biochem.* 35, 353–363. doi:10.1159/000369701

Dagher, Z., Garçon, G., Billet, S., Gosset, P., Ledoux, F., Courcot, D., et al. (2006). Activation of different pathways of apoptosis by air pollution particulate matter (PM2.5) in human epithelial lung cells (L132) in culture. *Toxicology* 225, 12–24. doi:10.1016/j.tox.2006.04.038

D'Anglemont de Tassigny, A., Souktani, R., Henry, P., Ghaleh, B., and Berdeaux, A. (2004). Volume-sensitive chloride channels (ICl, vol) mediate doxorubicin-induced apoptosis through apoptotic volume decrease in cardiomyocytes. *Fundam. Clin. Pharm.* 18, 531–538. doi:10.1111/j.1472-8206.2004.00273.x

Dinoi, A., Gulli, D., Ammoscato, I., Calidonna, C. R., and Contini, D. (2021). Impact of the coronavirus pandemic lockdown on atmospheric nanoparticle concentrations in two sites of Southern Italy. *Atmosphere* 12, 352. doi:10.3390/atmos12030352

Foster, K. A., Oster, C. G., Mayer, M. M., Avery, M. L., and Audus, K. L. (1998). Characterization of the A549 cell line as a type II pulmonary epithelial cell model for drug metabolism. *Exp. Cell Res.* 243, 359–366. doi:10.1006/excr.1998.4172

Friard, J., Laurain, A., Rubera, I., and Duranton, C. (2021). LRRC8/VRAC channels and the redox balance: A complex relationship. *Cell. Physiol. biochem.* 55, 106–118. doi:10.33594/000000341

Gelles, J. D., Mohammed, J. N., Santos, L. C., Legarda, D., Ting, A. T., and Chipuk, J. E. (2019). Single-cell and population-level analyses using real-time kinetic labeling couples proliferation and cell death mechanisms. *Dev. Cell* 51, 277–291.e4. doi:10.1016/j.devcel.2019.08.016

Ghio, A. J., Carraway, M. S., and Madden, M. C. (2012). Composition of air pollution particles and oxidative stress in cells, tissues, and living systems. *J. Toxicol. Environ. Health B Crit. Rev.* 15, 1–21. doi:10.1080/10937404.2012.632359

Giordano, M. E., Caricato, R., and Lionetto, M. G. (2020). Concentration dependence of the antioxidant and prooxidant activity of trolox in HeLa cells: Involvement in the

induction of apoptotic volume decrease. *Antioxidants* 2020, 1058. doi:10.3390/antiox9111058

Guascito, M. R., Lionetto, M. G., Mazzotta, F., Conte, M., Giordano, M. E., Caricato, R., et al. (2023). Characterisation of the correlations between oxidative potential and *in vitro* biological effects of PM10 at three sites in the central Mediterranean. *J. Hazard. Mat.* 448, 130872. doi:10.1016/j.jhazmat.2023.130872

Han, X., and Zhuang, Y. (2021). PM$_{2.5}$ induces autophagy-mediated cell apoptosis via PI3K/AKT/mTOR signaling pathway in mice bronchial epithelium cells. *Exp. Ther. Med.* 21, 1. doi:10.3892/etm.2020.9433

He, W., Li, H., Min, X., Liu, J., Hu, B., Hou, S., et al. (2010). Activation of volume-sensitive Cl$^-$ channel is involved in carboplatin-induced apoptosis in human lung adenocarcinoma cells. *Cancer Biol. Ther.* 9, 885–891. doi:10.4161/cbt.9.11.11666

Hoffmann, E. K., Sørensen, B. H., Sauter, D. P., and Lambert, I. H. (2015). Role of volume-regulated and calcium-activated anion channels in cell volume homeostasis, cancer and drug resistance. *Channels* 9, 380–396. doi:10.1080/19336950.2015.1089007

Jiao, J. D., Xu, C. Q., Yue, P., Dong, D. L., Li, Z., Du, Z. M., et al. (2006). Volume-sensitive outwardly rectifying chloride channels are involved in oxidative stress-induced apoptosis of mesangial cells. *Biochem. Biophys. Res. Commun.* 340, 277–285. doi:10.1016/j.bbrc.2005.11.175

Kannan, K., and Jain, S. K. (2000). Oxidative stress and apoptosis. *Pathophysiology* 7, 153–163. doi:10.1016/s0928-4680(00)00053-5

Kokubun, S., Saigusa, A., and Tamura, T. (1991). Blockade of Cl$^-$ channels by organic and inorganic blockers in vascular smooth muscle cells. *Pflugers Arch.* 418, 204–213. doi:10.1007/BF00370515

Lee, E. L., Shimizu, T., Ise, T., Numata, T., Kohno, K., and Okada, Y. (2007). Impaired activity of volume-sensitive Cl$^-$ channel is involved in cisplatin resistance of cancer cells. *J. Cell Physiol.* 211, 513–521. doi:10.1002/jcp.20961

Leventis, P. A., and Grinstein, S. (2010). The distribution and function of phosphatidylserine in cellular membranes. *Annu. Rev. Biophys.* 39, 407–427. doi:10.1146/annurev.biophys.093008.131234

Lionetto, M. G., Giordano, M. E., Calisi, A., Caricato, R., Hoffmann, E., and Schettino, T. (2010). Role of BK channels in the apoptotic volume decrease in native eel intestinal cells. *Cell. Physiol. biochem.* 25, 733–744. doi:10.1159/000315093

Lionetto, M. G., Guascito, M. R., Caricato, R., Giordano, M. E., De Bartolomeo, A. R., Romano, M. P., et al. (2019). Correlation of oxidative potential with ecotoxicological and cytotoxicological potential of PM$_{10}$ at an urban background site in Italy. *Atmosphere*, 10, 733. doi:org/doi:10.3390/atmos10120733

Lionetto, M. G., Guascito, M. R., Giordano, M. E., Caricato, R., De Bartolomeo, A. R., Romano, M. P., et al. (2021). Oxidative potential, cytotoxicity, and intracellular oxidative stress generating capacity of PM$_{10}$: A case study in South of Italy. *Atmosphere.* 12, 464. doi:org/doi:10.3390/atmos12040464

Loomis, D., Grosse, Y., Lauby-Secretan, B., Ghissassi, F. E., Bouvard, V., Benbrahim-Tallaa, L., et al. (2013). The carcinogenicity of outdoor air pollution. *Lancet Oncol.* 14, 1262–1263. doi:10.1016/s1470-2045(13)70487-x

Maeno, E., Ishizaki, Y., Kanaseki, T., Hazama, A., and Okada, Y. (2000). Normotonic cell shrinkage because of disordered volume regulation is an early prerequisite to apoptosis. *Proc. Natl. Acad. Sci. U. S. A.* 97, 9487–9492. doi:10.1073/pnas.140216197

Matsuda, J. J., Filali, M. S., Moreland, J. G., Miller, F. J., and Lamb, F. S. (2010). Activation of swelling-activated chloride current by tumor necrosis factor-alpha requires ClC-3-dependent endosomal reactive oxygen production. *J. Biol. Chem.* 285, 22864–22873. doi:10.1074/jbc.M109.099838

Okada, Y., Shimizu, T., Maeno, E., Tanabe, S., Wang, X., and Takahashi, N. (2006). Volume-sensitive chloride channels involved in apoptotic volume decrease and cell death. *J. Membr. Biol.* 209, 21–29. doi:10.1007/s00232-005-0836-6

Okada, Y., Maeno, E., Shimizu, T., Dezaki, K., Wang, J., and Morishima, S. (2001). Receptor-mediated control of regulatory volume decrease(RVD) and apoptotic volume decrease (AVD). *J. Physiol.* 532, 3–16. doi:10.1111/j.1469-7793.2001.0003g.x

Okada, Y., Sabirov, R. Z., Sato-Numata, K., and Numata, T. (2021). Cell death induction and protection by activation of ubiquitously expressed anion/cation channels. Part 1: Roles of VSOR/VRAC in cell volume regulation, release of double-edged signals and apoptotic/necrotic cell death. *Front. Cell Dev. Biol.* 8, 614040. doi:10.3389/fcell.2020.614040

Peixoto, M. S., de Oliveira Galvão, M. F., and Batistuzzo de Medeiros, S. R. (2017). Cell death pathways of particulate matter toxicity. *Chemosphere* 188, 32–48. doi:10.1016/j.chemosphere.2017.08.076

Poulsen, K. A., Andersen, E. C., Klausen, T. K., Hougaard, C., Lambert, I. H., and Hoffmann, E. K. (2010). Deregulation of apoptotic volume decrease and ionic movements in multidrug resistant tumor cells: Role of the chloride permeability. *Am. J. Physiol.* 298, C14–C25. doi:10.1152/ajpcell.00654.2008

Redza-Dutordoir, M., and Averill-Bates, D. A. (2016). Activation of apoptosis signalling pathways by reactive oxygen species. *Biochim. Biophys. Acta* 1863, 2977–2992. doi:10.1016/j.bbamcr.2016.09.012

Romano, S., Perrone, M. R., Becagli, S., Pietrogrande, M. C., Russo, M., Caricato, R., et al. (2020). Ecotoxicity, genotoxicity, and oxidative potential tests of atmospheric PM10 particles. *Atmos. Environ.* 221, 117085. doi:10.1016/j.atmosenv.2019.117085

Shen, M., Wang, L., Wang, B., Wang, T., Yang, G., Shen, L., et al. (2014). Activation of volume-sensitive outwardly rectifying chloride channel by ROS contributes to ER stress and cardiac contractile dysfunction: Involvement of CHOP through wnt. *Cell Death Dis.* 5, e1528. doi.org/doi:10.1038/cddis.2014.479

Shimizu, T., Numata, T., and Okada, Y. (2004). A role of reactive oxygen species in apoptotic activation of volumesensitive Cl$^-$ channel. *Proc. Natl. Acad. Sci. U. S. A.* 101, 6770–6773. doi:10.1073/pnas.0401604101

Wang, B., Li, K., Jin, W., Lu, Y., Zhang, Y., Shen, G., et al. (2013). Properties and inflammatory effects of various size fractions of ambient particulate matter from Beijing on A549 and J774A.1 cells. *Cells. Environ. Sci. Technol.* 47, 10583–10590. doi:10.1021/es401394g

Wei, H., Yuan, W., Yu, H., and Geng, H. (2021). Cytotoxicity induced by fine particulate matter (PM2.5) via mitochondria-mediated apoptosis pathway in rat alveolar macrophages. *Environ. Sci. Pollut. Res. Int.* 28, 25819–25829. doi:10.1007/s11356-021-12431-w

WHO (2019). *Noncommunicable disease and air pollution. WHO European high-level conference on noncommunicable diseases.* Copenhagen, Denmark: WHO Regional Office for Europe.

Yang, L., Liu, G., Fu, L., Zhong, W., Li, X., and Pan, Q. (2020). DNA repair enzyme OGG1 promotes alveolar progenitor cell renewal and relieves PM2.5-induced lung injury and fibrosis. *Ecotoxicol. Environ. Saf.* 205, 111283. doi:10.1016/j.ecoenv.2020.111283

Yang, X., Feng, L., Zhang, Y., Hu, H., Shi, Y., Liang, S., et al. (2018). Cytotoxicity induced by fine particulate matter (PM2.5) via mitochondria-mediated apoptosis pathway in human cardiomyocytes. *Ecotoxicol. Environ. Saf.* 161, 198–207. doi:10.1016/j.ecoenv.2018.05.092

Yi, S., Zhang, F., Qu, F., and Ding, W. (2012). Water-insoluble fraction of airborne particulate matter (PM10) induces oxidative stress in human lung epithelial A549 cells. *Environ. Toxicol.* 29, 226–233. doi:10.1002/tox.21750

Yu, S. P., and Choi, D. W. (2000). Ions, cell volume, and apoptosis. *Proc. Natl. Acad. Sci. U. S. A.* 97, 9360–9362. doi:10.1073/pnas.97.17.9360

Zhang, J., Liu, J., Ren, L., Wei, J., Duan, J., Zhang, L., et al. (2018). PM$_{2.5}$ induces male reproductive toxicity via mitochondrial dysfunction, DNA damage and RIPK1 mediated apoptotic signaling pathway. *Sci. Total Environ.* 634, 1435–1444. doi:10.1016/j.scitotenv.2018.03.383